

## DIELECTRIC RELAXATION OF TGS CRYSTAL IN THE SECOND ORDER PHASE TRANSITION

HORIA V. ALEXANDRU\*, CARMEN MINDRU, C. BERBECARU  
*Faculty of Physics, University of Bucharest, Romania*

Pure triglycine sulphate crystals (TGS for short) undergo a second order phase transition around 49 °C. Peculiar dielectric dispersion of TGS has been noticed walking up and down the temperature through the Curie Point. The dielectric measurements were made on the frequency range 45 Hz ÷ 5 MHz, between 65 °C and -150 °C. The Cole-Cole representation of the two- component of permittivity shows two types of relaxation in the ferroelectric phase, crossing down the Curie Point. The temperature and frequency dependence of both components of permittivity was investigated. The slope ratio of the reverse of permittivity in ferro and in paraelectric phase shows a 'strange' frequency dependence. An unusual slope change of this ratio was found in the frequency range (1-5)·10<sup>5</sup> Hz. This peculiar dependence does not have a straightforward explanation and seems to be for the first time related in the literature.

(Received August 14, 2012; Accepted September 6, 2012)

*Keywords:* Triglycine sulphate, permittivity relaxation, dielectric spectroscopy

### 1. Introduction

Ferroelectric TGS crystal has been extensively studied both in pure state and doped. Fundamental ferroelectric properties were earlier studied [1]. Several applications of this crystal have been found as pyroelectric detector in electronics [2], candidate ferroelectric data storage devices (nonvolatile memories) and nanofabrication. These applications require fundamental studies of dynamic and structure domain as well as special studies of polarization switching phenomena, even at the nanoscale. Relevant studies have been performed in the field of ferroelectric crystals [3, 4], lattice dynamics [5, 6] and dielectric relaxation [7-9].

Hoshino et al [10] first studied the structure of triglycine sulphate crystals and essential ferroelectric parameters were revealed [11].

We have previously published the growth conditions and properties of pure and doped TGS crystals [12-15]. Zhang had performed Cole-Cole [16] analysis at lower temperatures and carefully around the Curie Point [3, 17].

### 2. Experimental

Triglycine sulphate crystals were grown from solution, by slow solvent evaporation in a thermostated oven at 52 °C, i.e. in the paraelectric phase. Plates of ~ 1 mm thick were cleaved perpendicular to the b-ferroelectric axis, were grounded, polished and silver electrodes were painted. The TGS sample of about 0.8 cm<sup>2</sup> surface was fitted in a special holder for measurements, placed in a special oven. Heating/cooling of this oven, between RT and 65 °C, was monitored with a constant temperature variation. Cooling down to -150 °C of the sample holder was performed in a special chamber with vapors of liquid nitrogen. In order to avoid water condensation on the

---

\*Corresponding author: horia@infim.ro

sample (the dew point), a nitrogen stream was continuously gently flown through the sample holder. Chromel–alumel thermocouple and Kethley 2010 voltmeter have been used for temperature control of the sample.

HIOKI 3532-50 RLC automatic bridge was used for dielectric measurements, monitored by the computer through the GPIB interface. Dielectric parameters and temperature were explored in continuous repeated cycles (of about one minute) for a number of beforehand chosen frequencies between 45 Hz and 5 MHz.

Measurements have been performed in three temporal stages (step I, step II and step III), one week break time between them, as shown in fig.1. Data collected by decreasing the temperature in step II and step III, i.e. segment 4 and 5 will be analyzed in this paper.

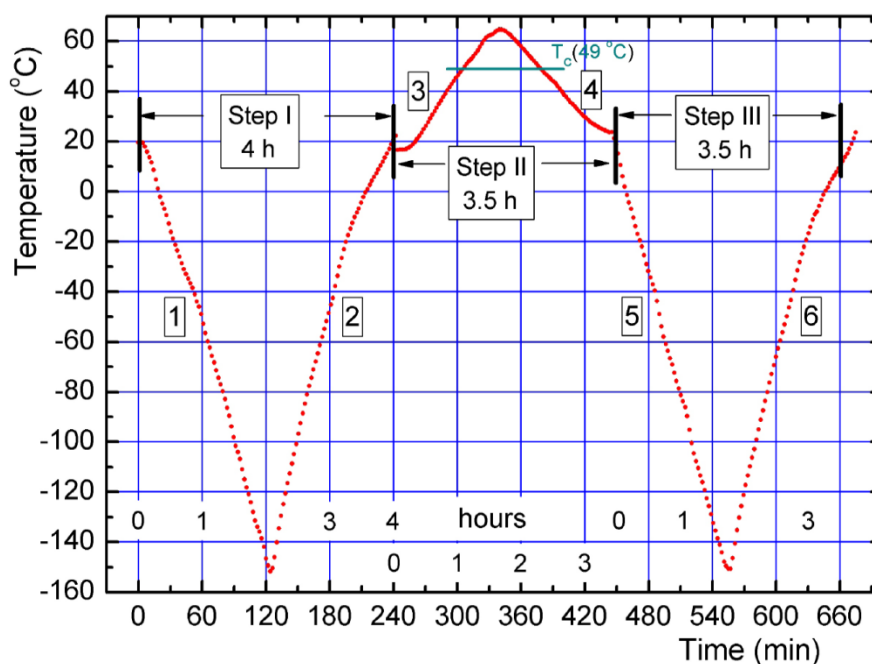


Fig.1. Time - Temperature chart measurements of the dielectric parameters, in three temporal stages.

In the step I, on the segment 1 and 2, the temperature excursion down to  $-150^{\circ}\text{C}$  and back to RT do not show important differences of the dielectric parameters one versus the other. However, the permittivity components on the similar temperature variation segment 5-6, show much higher values than on the segment 1-2 (not all data are presented in fig.2).

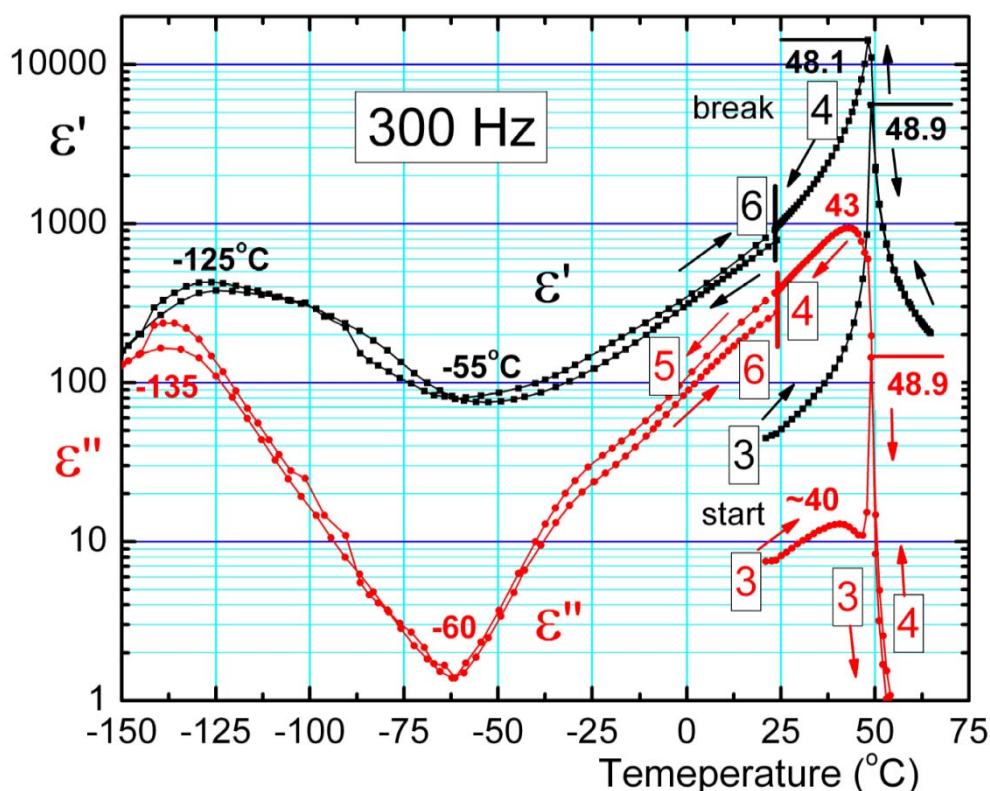


Fig.2. Temperature dependence of the permittivity components at the frequency of 300 Hz, along the routes presented in fig.1. (Routes 1 and 2 of much smaller permittivity values were omitted).

In the step II (fig.1), the temperature crosses up the CP, reaches 65 °C and then get down to room temperature (RT). After a week-time break, the temperature was decreased again from RT to -150 °C (segment 5) and then raised to RT (segment 6). Remarkable differences of the permittivity components have been found on the segment 4 versus the segment 3 (see fig.2) and on the segment 5/6 versus segment 1/2 (not all data are presented here).

In fig.1, the rate of the temperature decrease was 0.53 °C/min on the segment 4 and 1.60 °C/min on the segment 5. The two components of permittivity were estimated from measured capacity and losses.

In fig.3, the two components of permittivity have been represented versus frequency at 47 °C, in the ferroelectric phase, i.e. about two Celsius degree lower than the transition temperature (Curie Point). The two-relaxation mechanisms have appeared, at lower and higher frequencies, very close to the values found in ref. [18].

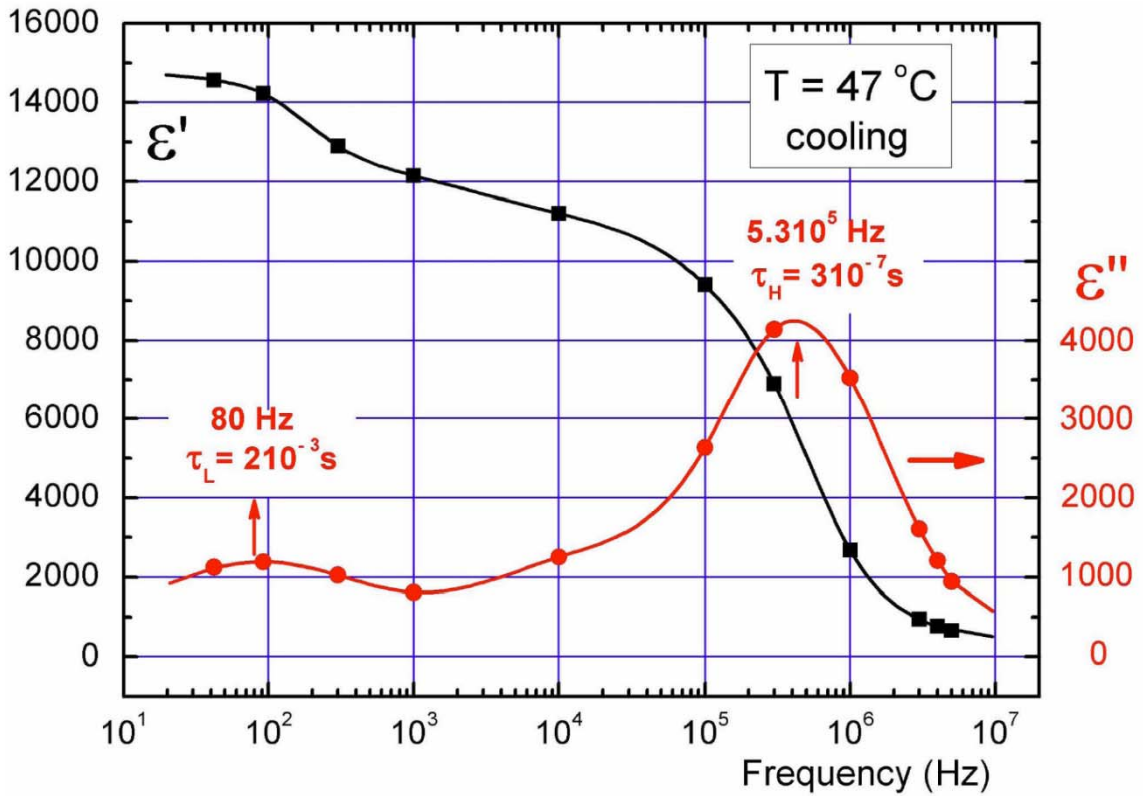


Fig.3. Frequency dependence of the real and imaginary component of permittivity. Two distinct relaxation mechanism at lower ~80 Hz and at higher frequencies ~530 kHz have appeared in ferroelectric phase, about 2 °C lower than Curie Point.

Specific notation of the two relaxation mechanisms according to Cole-Cole (C-C) model [16] is drawn in fig.4. The circles radius has a specific angle  $\alpha\pi/2$  with the abscissa, for higher and lower frequencies relaxation mechanism.

**Cole – Cole parameters representation.**

Low frequencies	$\epsilon'_{Lmin}$	$\epsilon'_{Lmax}$	$\Delta\epsilon'_L/2$	$\Delta y_L$	$\epsilon''_{Lmax}$	$\epsilon'_L$	$R_L$
High frequencies	$\epsilon''_{Hmin}$	$\epsilon''_{Hmax}$	$\Delta\epsilon'_H/2$	$\Delta y_H$	$\epsilon''_{Hmax}$	$\epsilon'_H$	$R_H$

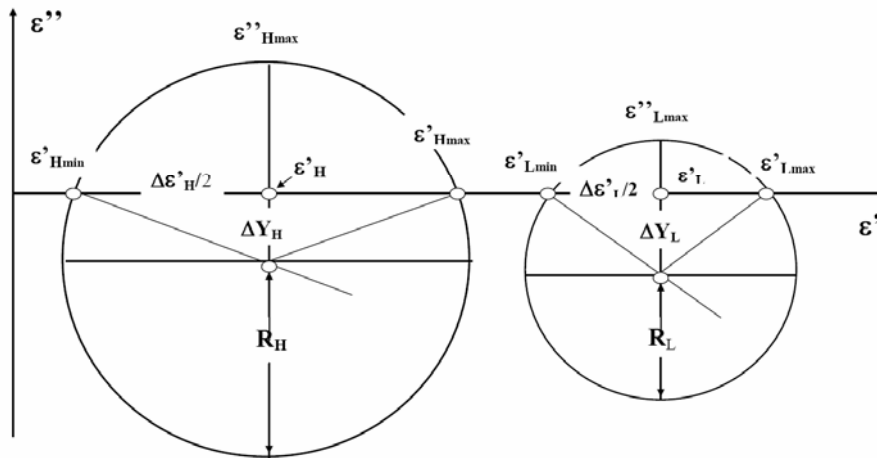


Fig.4. Cole-Cole parameters scheme for two relaxation mechanisms at lower (L index) and higher (H index) relaxation frequencies, at a given temperature.

In Cole-Cole [16] representation,  $\epsilon''$  vs.  $\epsilon'$  in fig.5, shows also two relaxation mechanisms at lower ( $\sim 100$  Hz) and at higher (MHz) frequencies. All-important parameters, like  $\alpha$  C-C parameters, min. and max. values of  $\epsilon'$ , relaxation frequencies corresponding to the highest values of  $\epsilon''$ , can be much easily and much more precisely evaluated (see ref. [18]).

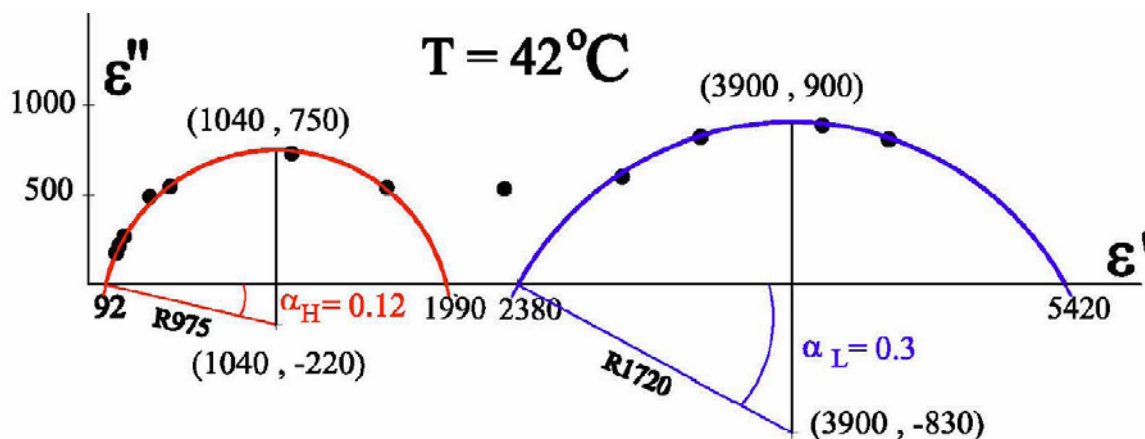


Fig.5. Cole-Cole real parameters representation ( $\epsilon''$  vs.  $\epsilon'$ ) at  $42^\circ\text{C}$ . The highest values of  $\epsilon''$  on the circles correspond to the relaxation frequency (and relaxation time – see below) of the two mechanism of relaxation.

### 3. Results

#### 3.1. Temperature and frequency dependence of permittivity components.

The real  $\epsilon'$  and the imaginary  $\epsilon''$  components of permittivity vs. frequency, on the segment 5 (fig.1), at  $47^\circ\text{C}$ , in the ferro phase near the CP are presented in fig.3. The peak values of  $\epsilon''$  are correlated with the stepwise decrease of  $\epsilon'$ . The relaxation time associated with the two relaxation mechanisms are  $\tau_L \approx 2$  msec at lower and  $\tau_H \approx 0.3$   $\mu\text{sec}$  at higher frequencies. However, the C-C representations (fig.5) offer a much higher precision in estimation of these parameters.

In fig. 2, we present the temperature dependence of both components of permittivity at the frequency of 300 Hz. Up and down temperature excursion, between RT and  $-150^\circ\text{C}$ , i.e. segments 5 and 6 of both components of permittivity, does not show significant differences.

A large difference of more than one order of magnitude of both components of permittivity, was noticed in up and down temperature excursion between RT and  $65^\circ\text{C}$  (segment 3 and 4 in fig.2). The estimated values of permittivity components and their ratio on the segment 4 vs. the segment 3, in the ferroelectric phase, are presented in table 1. The mean value of  $\epsilon'$  and  $\epsilon''$  ratio on the segment 4 vs. segment 3 is approximately 22 and 65 respectively, on a large temperature range between  $25$  and  $45^\circ\text{C}$ . However, between  $45^\circ\text{C}$  and the CP this ratio decreases dramatically (see line  $T_c$  in table 1), showing that a special mechanism of ferroelectric domains evolution take place in this region.

Table 1. Selected values of the real and imaginary component of permittivity on the segment 3 and 4, step II, in fig. 2.

T (°C)	$\epsilon'$			$\epsilon''$		
	Segment [3]	Segment [4]	Ratio [4] / [3]	Segment [3]	Segment [4]	Ratio [4] / [3]
25	51	1020	20	8	400	50
35	90	1950	21.7	11.5	700	61
40	130	3030	23.3	12.9	890	69
45	270	6160	22.8	11.1	900	81
Tc	5500	14200	2.6	143	~200	1.4
	<b>Mean ratio value <math>\Rightarrow</math></b>		<b>22 <math>\pm</math> 2</b>	<b>Mean ratio value <math>\Rightarrow</math></b>		<b>65 <math>\pm</math> 15</b>

The imaginary component of permittivity shows a peculiar behavior between 40 °C and the Curie Point. Walking up and down the temperature, the imaginary component  $\epsilon''$ , always has a large secondary maxima on this temperature range, besides of its usual maxima at the CP. The position of this 'secondary maxima' is frequency dependent and was also noticed in the literature (see fig.4 in ref [20]). The explanation of this 'secondary maxima' is still lacking in the literature.

The maximum value of both component of permittivity around -130 °C, was considered as a low-temperature phase transition, using Raman and ultrasonic measurements [19]. In fact, our full dielectric measurements show that the temperature position of this maxima depends on the frequency and the phenomenon seems to me much more complicated, but not necessary related to a real transition.

### 3.2. Cole-Cole representation.

We shall introduce the notations:  $\Delta\epsilon'_H = \epsilon'_{Hmax} - \epsilon'_{Hmin}$  and  $\Delta\epsilon'_L = \epsilon'_{Lmax} - \epsilon'_{Lmin}$ , according to fig.4, at high and low frequency relaxations. Analysis of the experimental data of dielectric spectroscopy, is usually accomplished with Cole-Cole [16], general equation:

$$\epsilon^*(\omega) - \epsilon_\infty = \frac{\epsilon_S - \epsilon_\infty}{1 + (i\omega\tau_\epsilon)^{1-\alpha}} \quad (1)$$

The  $\alpha_H$ ,  $\alpha_L$  Cole-Cole parameters and the relaxation times  $\tau_H$  and  $\tau_L$  for high and low relaxation are very important parameters to be considered.

Experimental permittivity data in C-C representation at 42 °C, are presented in fig. 5. High and low frequency parameters were estimated from such figures, according to the parameter nominations in fig.4. In our experiments we do not have Debye (unique relaxation time) representations, but C-C, with a distribution of relaxation time for both mechanisms, larger for the lower frequencies ones ( $\alpha_H < \alpha_L$ ). The main relaxation times  $\tau_H$  and  $\tau_L$  can be found from conditions  $\omega\tau = 1$ , i.e.  $\tau = 1 / 2\pi f_{relax}$ , written for  $f_{relax}$  corresponding to the  $\epsilon''$  maximum values in the fig.5 types.

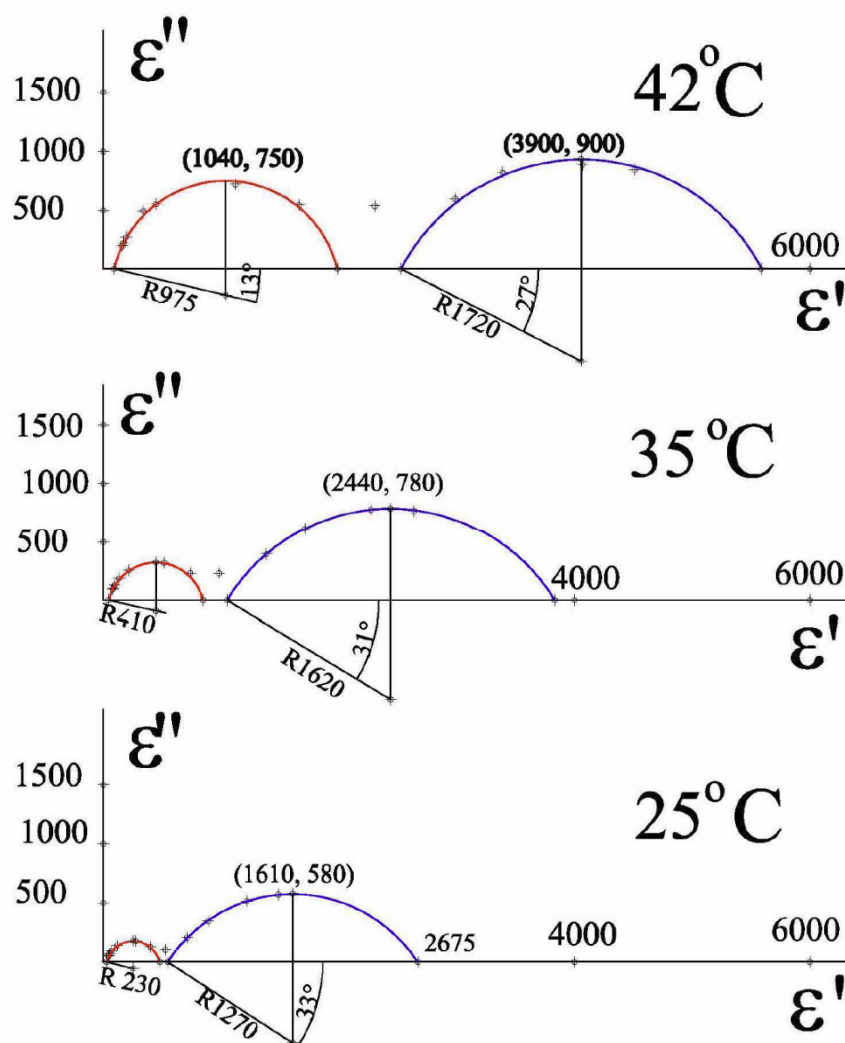


Fig.6. Cole-Cole representation of permittivity components at given temperatures. The radius of the arcs C-C decreases slowly with the temperature decrease, but much more rapidly for higher frequency mechanism

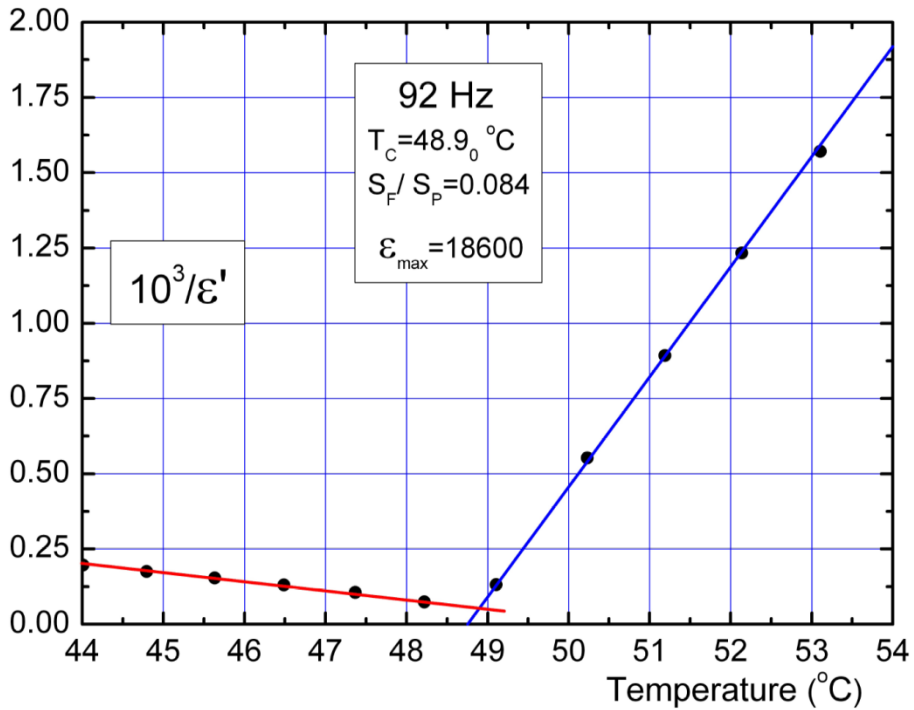
Fig. 6 shows a set of Cole-Cole representations at the same scale, for several temperatures lower than CP. There is a continuous decrease of the radius of both types of arc C-C with the temperature decrease. However, the radius of the higher frequency relaxation mechanism steeply decreases in this temperature range, but keeps  $\tau_H$  almost constant (see fig.8 in ref. [18]). The C-C parameter of the low frequency relaxation mechanism  $\alpha_L$  is much larger than for higher frequency mechanism, i.e. the distribution of the relaxation time  $\tau_L$  is much larger.

### 3.3. Curie-Weiss law at the ferroelectric transition.

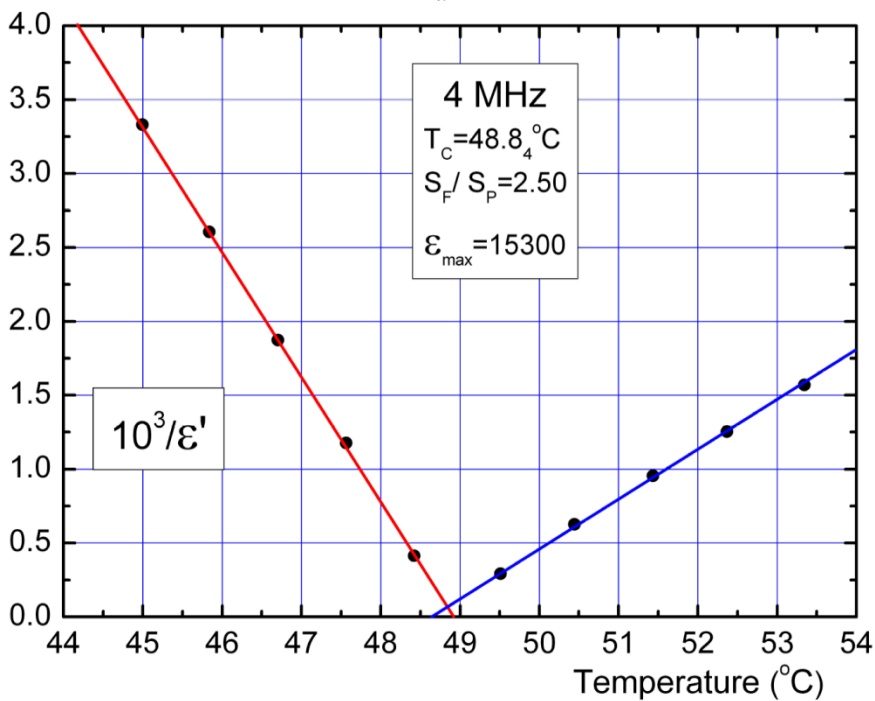
According to the thermodynamic and Landau theory, the ratio of the slope of  $1/\epsilon'$  in ferro vs. paraelectric phase, has to be two. Experimental evaluation of this ratio was found higher than two, even in the microwave region, where Luther [7], has estimated this ratio to be 4.75

The value of this ratio was estimated in the literature (see also Landolt-Börnstein [1]) only when the temperature increases, i.e. when the ferroelectric topography of the domain is quite stable. The question is: what happened with this ratio when the temperature increases and then decreases, crossing down the CP? To the best of our knowledge, this problem was not really approached. The reason is probably the metastable state, which appears crossing down the CP in the ferroelectric state and the uncontrolled increase of both components of permittivity, as previously shown (see fig.2).

In our case, on the segment 4 (step II, in fig.1),  $1/\epsilon'$  the reverse of the real component of permittivity, in ferro and in para phases, at two distinct (extreme) frequencies 92 Hz and 4 MHz are presented in figs. 7.a and 7.b (see also table 2). The slope of  $(1/\epsilon')_{\text{para}}$  in paraelectric phase is quite the same for all frequencies we have measured. However, the ferro phase, slope of  $(1/\epsilon')_{\text{ferro}}$  in table 2 increases more than one order of magnitude at higher frequencies.



a



b

Fig.7.a.b. The reverse of permittivity and the slope ratio at the frequency: a/ 92 Hz and b/ 4 MHz.

Table 2. Slope evaluation of the reverse permittivities and their ratio at two extreme frequencies.

Frequency	Slope( $1/\varepsilon''$ ) <sub>ferro</sub>	Slope( $1/\varepsilon''$ ) <sub>para</sub>	$S_f / S_p$
92 Hz	$30.7 \cdot 10^{-6}$	$360 \cdot 10^{-6}$	0.084
4 MHz	$843 \cdot 10^{-6}$	$340 \cdot 10^{-6}$	2.50

In order to make clear this aspect, we have drawn in fig.8 the slope ratio  $S_{\text{ferro}}/S_{\text{para}}$  versus frequency on heating (zone 3, as usually) and on cooling (zone 4).

The graphic in fig.8 offers puzzling results. On heating (zone 3), the slope ratio is about 2.9 at 1 kHz, which is quite usually and increases very slowly up to the frequency of  $\sim 10^5$  Hz. At higher frequencies, the slope ratio increases rapidly up to the higher limit of frequency 5 MHz. On cooling (zone 4), the slope ratio is less than 0.1 at 1 kHz and again, unusually, increases very rapidly at frequencies higher than  $\sim 5 \cdot 10^5$  Hz. The equations of the slope ratio  $S_{\text{ferro}}/S_{\text{para}}$  dependence on frequency are presented in table 3. The higher value of the ratio dependences, extrapolated crosses each other around 50 MHz, at the slope ratio of about five. Other aspects will be further discussed.

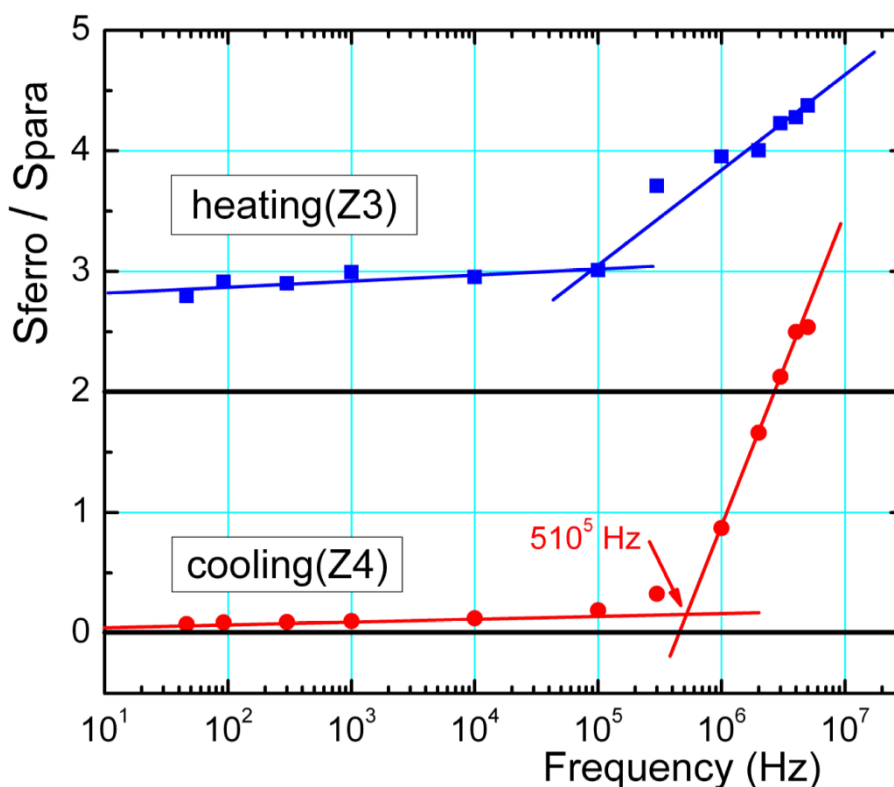


Fig.8. The frequency dependence of the slope ratio of the reverse of permittivity in ferro vs, para phase. The frequency dependences of these ratios on heating and on cooling, in semilog scale are given in table 3.

Table 3. The slope ratios  $S_{ferro}/S_{para}$  of the reverse of permittivity, versus frequency on heating (Zone 3) and on cooling (Zone 4). Higher frequencies extrapolated dependences cross each other around 50 MHz.

	Low frequencies	High frequencies
Heating (Z3)	$S_f / S_p = 2.8 + 0.048 \log v$	$S_f / S_p = - 0.92 + 0.79 \log v$
Cooling (Z4)	$S_f / S_p = 0.018 + 0.024 \log v$	$S_f / S_p = - 14.7 + 2.6 \log v$

Crosses each other at 44 MHz (~50 MHz) and  $y=5.1$

#### 4. Discussions

Dielectric spectroscopy measurements, performed on a large frequency range, have revealed unusual aspects of the dielectric relaxation, of the TGS crystal. There are two relaxation mechanisms: “the critical slowing down”, at higher frequency (MHz range), whose relaxation time is not influenced by temperature (see ref. [18]) and the relaxation of ferroelectric domains at lower (~100 Hz range) frequencies.

Temperature dependence of the permittivity components show a large maxima at lower temperatures (around -130 °C, see fig.2), which might suggest a new transition [19]. In fact, the frequency dependence of the position of this maxima, might probably suggest some other effects in the structure of TGS crystal.

At the ferroelectric transition (~49 °C), walking up and then down the temperature through the Curie Point, both permittivity components increase more than one order of magnitude. Crossing down the CP, appears a metastable ferroelectric state. On the temperature range 25-45 °C the real permittivity component increases ~22 times and the imaginary one increases ~65 times versus the values measured with the temperature increase (see table 1). On the temperature range 45 °C ÷  $T_C$  there is a much smaller increase of the permittivity.

The metastable state of TGS crystal, following our experience, has a long period of “relaxation”. The permittivity, gets its minimum stable value only after several weeks.

In the second order ferroelectric transition, “polarization”, the order parameter, increases just from zero to unusual higher values when the temperature crosses down the CP. The ferroelectric domains nucleate in the lattice on charged defects at the nanometric scale and extend to micro and then, more or less rapidly, to the macroscopic scale dimensions.

Punctual charged defects, like Frenkel and Schottky and even larger dimension defects like dislocations, initiate the birth of the ferroelectric domains. The punctual defects have a statistical nature and a temperature activated distribution. The concentration of dislocations and of other extended defects depends on the crystal perfection and there are not of thermodynamic equilibrium, depending on the mechanical, thermal strength, etc.

In fact, experimental observations [21-23] have shown that at nano and micro scale, after crossing down the CP, a huge number of ferroelectric domains appear. It follows a period of domains cropping. The larger domains “engulf” the smaller ones by ferroelectric domain walls movement. Several fences, lattice defects, including dislocations, impede the walls displacement and slowly stabilize the structure. Thus, crossing down the CP, the topography evolution of nanometer, just born domain nuclei, make a long-term metastable state in pure ferroelectric crystals.

In the permittivity measurements, even at very small electric field applied (less than 1 V/cm), the contribution of the domain walls “oscillation” can exceed 80% of the registered permittivity [4]. Then, the number of ferroelectric domains and consequently the whole length of the domain walls has a notorious influence on the dielectric measurements.

The temporal evolution of the topography of the ferroelectric domains was revealed in the literature, whereas the metastable state evolution of permittivity was not. The main reason might be the non-reproducible character of this evolution, depending on the temperature, speed evolution and the sample characteristics (defect concentrations mainly).

However, even in this condition, our results revealed by dielectric spectroscopy, have shown very interesting aspects. Studies of frequency and temperature measurements, that characterize the metastable state of TGS crystal, offered plenty of interesting data.

One interesting aspect is the evolution of the ratio of the reverse permittivity ( $1/\varepsilon'$ ) in ferro versus para phase, on the first run (temperature increase), compared to second one (temperature decrease), in relation with the frequency. In fig. 7.a and 7.b are illustrated the Curie-Weiss law at some extreme measured frequencies. The extremely small slope ratio, on cooling, of about 0.084 is puzzling.

In fig. 8 we have drawn the frequency dependence of the slopes ratio  $S_{\text{ferro}}/S_{\text{para}}$ , on heating and on cooling runs. The theoretical reference value 2, is also drawn as reference. On heating, the slope ratio close to value 3, is not unusual. However, the sudden increase of the slope of the linear dependence of this ratio, at frequencies higher than  $\sim 10^5$  Hz, is quite unexpected. In the cooling run (fig. 8), the mentioned aspect repeats again around the frequency of about  $5 \cdot 10^5$  Hz (see also table 3). The unusually small slope ratio, of about 0.1 at lower frequencies, correlates with the steeper increase of permittivity on the segment 4, in fig.2 (see also table 1).

The sudden increase of the slope ratio starting at  $10^5$  Hz, might be related to the piezoelectric effect of the TGS lattice in the ferroelectric phase. Indeed, Fousek and Janousek [4] have found the piezoelectric resonance of TGS plates, somewhere around 100 kHz. But checking the effect for TGS samples of several dimensions, varying more than one order of magnitude, it was found that the resonance frequencies almost did not change.

In a separate experiment, authors [4] have found that after a temperature “excursion” up and down through the CP, the resonant frequency was changed from 0.46 MHz to 1,1 MHz. No explanation could be offered, but it is quite certain that the domain topography is involved.

## 5. Conclusions

1. Dielectric spectroscopy, on a large frequency and temperature range, reveals interesting data about the metastable state in ferroelectric crystals, when the temperature crosses down the Curie Point. Two relaxation mechanism of permittivity at higher (MHz range) and lower ( $\sim 100$  Hz) frequencies are typical for this metastable state, which has a long period of ‘relaxation’ (several weeks).

2. In the first stages of the metastable state in TGS crystal, both components of permittivity unusually increases more than one order of magnitude on the temperature range 25-45 °C. Much less, increases the permittivity on a narrow temperature range below the CP. This mechanism was discussed.

3. The Curie-Weiss law, in the first stages of the metastable state, is heavily affected. The slope ratio of the reverse of permittivity in ferro vs. para phase, predicted to be 2 by the theory, might attain values as low as 1/10.

4. The frequency dependence of the ratio  $S_{\text{ferro}}/S_{\text{para}}$  of the slope of the reverse of permittivities, shows an unusual increase around  $10^5$  Hz. Both families of experimental points behave similarly at higher frequency and apparently cross each other at  $\sim 50$  MHz. Apparently, this effect is related to the piezoelectric effect, a characteristic of TGS in the ferro state. However, some literature data deny the straightforward effect, because the piezo frequencies do not change with the crystal dimension.

### Acknowledgements

Romanian National Authority for Scientific Research supported this work under the strategic Grant POSDRU 88/ 1.5/ S / 56668.

### References

- [1] Landolt-Börnstein vol. 16, Ferroelectrics and Related Substances, Springer-Verlag, 1982,
- [2] S.B. Lang, D.K. Das-Gupta, *Ferroelectrics Rev.* **2**, 266 (2000).
- [3] J. Zhang, *Ferroelectrics*, **281**, 105 (2002).
- [4] J. Fousek, V. Janousek, *Phys. Stat. Sol.* **13**, 195 (1966).
- [5] Genowefa Slosareki, A Heuerf, H Zimmermannf and U Haeberlent *J. Phys.: Condens. Matter* **1**, 5931 (1989).
- [6] V. Tripadus, A. Radulescu, J. Pieper, A. Buchsteiner, A. Podlesnyak, S. Janssen, A. Serban *Chemical Physics* **322**, 323 (2006).
- [7] G. Luther, *Phys. Stat. Sol. (a)* **20**, 227 (1973).
- [8] H.-G. Unruh, H.-J. Wahl, *Phys. Stat. Sol. (a)* **9**, 119 (1972).
- [9] K. Kuramoto, H. Motegi, E. Nakamura, K. Kosaki, *J. Physical Society Japan*, **55**, 377 (1986).
- [10] S. Hoshino, Y. Okaya, R. Pepinsky, *Phys. Rev.* **115**, 323 (1959),
- [11] S. Hoshino, T. Mitsui, F. Jona, R. Pepinsky, *Phys. Rev.* **107**, 323 (1957).
- [12] H.V. Alexandru, C. Berbecaru, *Cryst. Res. Technol.* **30**, 307 (1995).
- [13] H.V. Alexandru, C. Berbecaru, *Ferroelectrics* **202**, 173 (1997).
- [14] H.V. Alexandru, C. Berbecaru, F. Stanculescu, L. Pintilie, I. Matei, M. Lisca *Sensors and Actuators A* **113**, 387 (2004)–392
- [15] H.V. Alexandru, *Annals New York Academy of Sciences* **1161**, 387 (2009).
- [16] K.S.Cole, R.H.Cole, *J. Chem. Phys.* **9**, 341 (1941) -351
- [17] J. Zhang, *Phys. Stat. Sol. (a)* **193**, 347 (2002) -356
- [18] C. Mîndru, C. P. Ganea, H. V. Alexandru, *J. Optoelectron. Adv. Mater.* **14**, 157 (2012).
- [19] F.Y.El-Eithan,A.R.Bates, W.Gough, D.J.Somerford, *J.Phys.: Condens. Matter* **4** L249 (1992).
- [20] J.Przeslawski, T.Iglesias, G.Lifante, J.A.Gonzalo, *Ferroelectric Letters* **18**, 75 (1994).
- [21] Noriyuki Nakatani, *Jap J Appl Physics* **24**, 1528 (1985).
- [22] R. Luthi, H. Haefke, W. Gutmannsbauer, E. Meyer, L. Howald, H.-J. Guntherodt *J. Vac. Sci. Technol. B* **12**, 2451 (1994).
- [23] N. Nakatani, *Jap J Appl Physics* **24**, L528 (1985).